Chemical Physics Letters 838 (2024) 141091

Contents lists available at ScienceDirect

Chemical Physics Letters

journal homepage: www.elsevier.com/locate/cplett

Research paper

VMC optimization of ultra-compact, explicitly-correlated wave functions of the Li isoelectronic sequence in its lowest 1s2s2p quartet state

D.J. Nader *, B.M. Rubenstein

Department of Chemistry, Brown University, Providence, RI 02912, United States

HIGHLIGHTS

- We illustrate the power of Variational Monte Carlo (VMC) to efficiently optimize explicitly correlated wave functions that accurately describe the quartet 1s2s2p state of the Li isoelectronic sequence with only ten parameters.
- We implement the gradient descent method to optimize the wave function, including non-linear variational parameters, which are typically challenging to optimize.
- We explore how the energy and non-linear variational parameters scale with the nuclear charge.

GRAPHICAL ABSTRACT

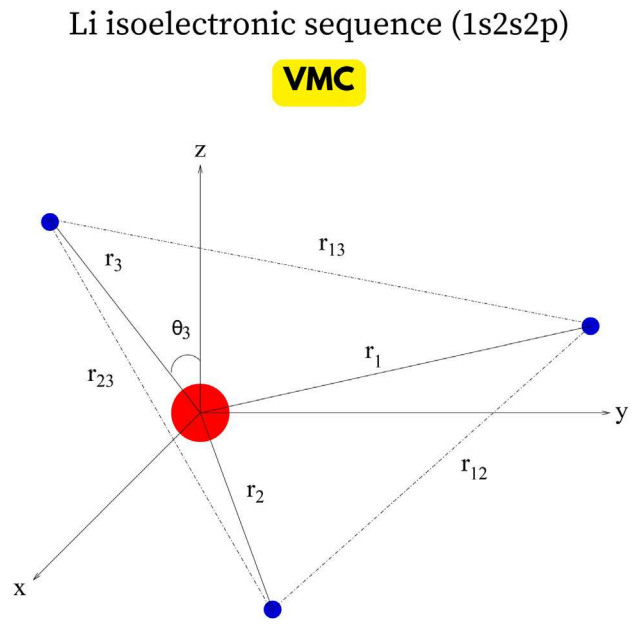

ARTICLE INFO

Dataset link: https://github.com/djuliannader/VMCLitio

Keywords:
Li isoelectronic series
Variational Monte Carlo
Explicitly-correlated wave functions

ABSTRACT

A compact yet accurate approach for representing the wave functions of members of the He and Li isoelectronic series is using explicitly correlated wave functions. These wave functions, however, often have nonlinear forms, which make them challenging to optimize. In this work, we show how Variational Monte Carlo (VMC) can efficiently optimize explicitly correlated wave functions that accurately describe the quartet $1s2s2p$ state of the Li isoelectronic sequence with ten or fewer parameters. We find that our compact wave functions correctly describe cusp conditions and reproduce at least 99.9% percent of the exact energy.

1. Introduction

The isoelectronic sequence of lithium, consisting of atoms with three electrons and a nucleus, is the simplest sequence of atomic systems

* Corresponding author.
E-mail addresses: daniel_nader@brown.edu (D.J. Nader), brenda_rubenstein@brown.edu (B.M. Rubenstein).

https://doi.org/10.1016/j.cplett.2024.141091
Received 25 October 2023; Received in revised form 28 December 2023; Accepted 15 January 2024
Available online 22 January 2024

that have both open and closed shell ground states, and thus serve as prototypes for the more complex ground states of heavier alkali-metal atoms and alkaline-earth cations [1]. The non-relativistic wave functions of atoms and ions with three electrons such as those in this sequence are also of great interest to those developing highly accurate evaluations of relativistic and QED corrections [2,3]. The Li isoelectronic sequence has therefore become a testbed for quantum chemical methods, much like He-like atoms were for many decades after the advent of quantum mechanics.

One particularly interesting state exhibited by members of this series is the $1s2s2p$ state, which is the lowest electronic state of the quartet manifold with total spin $S = 3/2$. Since optical quartet-to-doublet transitions are difficult to observe experimentally, the experimental uncertainty of this state is too large for it to be used in Grotrian diagrams [4]. This state of affairs has motivated researchers to develop more accurate electronic structure techniques and other means for determining the term values of this quartet state during the end of the last century [5]. The confirmation that a positron can be attached to this state to form e^+Li renewed interest in its electronic structure some years later [6–8]. Additionally, the $1s2s2p$ state is an eigenfunction of the angular momentum operators $\hat{L}^2$ and $\hat{L}_z$ with the eigenvalues $L(L+1) = 2$ and $M_L = 0$. Its ground state wave function is therefore not only a function of interelectronic distances (which would make its electronic structure problem into a six-dimensional problem), but is also dependent upon angular contributions that make it into a nine-dimensional problem.

Traditionally, the ground state of such species would be described using a single determinant with optimized orbitals or a multideterminant expansion with linear coefficients. Such linear expansions are often preferred because they lead to highly accurate energies, can be solved through standard linear algebra techniques, and automatically provide one with a physical picture of which electronic excitations contribute most to a state based upon the coefficients obtained. Previous works using linear expansions have provided benchmark energies for the $1s2s2p$ state: Conventional Configuration Interaction (CI) [5,9–11] with 2519 determinants and the Hylleraas method [12,13] with 1372 Hylleraas functions yielded energies with μHa accurate, as summarized in Ref. [14]. However, given the number of determinants that were needed to accurately describe this state, alternative approaches become attractive.

One set of alternative approaches are so-called explicitly-correlated approaches that attempt to find the "most compact" representations of wave functions, sometimes at the expense of overall accuracy [1,15–17].[1] Compact, yet accurate wave functions are particularly valuable if they accurately reproduce cusp conditions. From a practical point of view, explicitly-correlated compact wave functions are often used in the study of collisions [19–24] or to ease the computation of the matrix elements of the numerous singular operators representing relativistic and QED corrections [3]. One of the best approaches for designing compact wave functions is to include explicit correlation and use nonlinear variational parameters [25]. However, in contrast with conventional linear expansions in terms of determinants, the optimization of such wave functions is challenging since the optimal parameters cannot be found by solving the secular Schrödinger equation. The potentially large number of nonlinear parameters additionally presents a steep challenge for standard minimization algorithms.

Given this backdrop, a potentially promising technique for optimizing these challenging wave functions is the Variational Monte Carlo (VMC) method. In the VMC method, the parameters within a given wave function ansatz are optimized to minimize the energy by iteratively using Monte Carlo sampling to evaluate the energy for a given set of parameters and then finding an improved set of parameters that further minimize the energy [26,27]. While the energies given the parameters could be evaluated using traditional grid-based integration methods, this becomes more computationally costly than random sampling when eight or more dimensions are involved. Monte Carlo methods thus become the methods of choice for high dimensional search spaces [26]. Although VMC is most popularly used to optimize the Jastrow parameters within Slater–Jastrow wave functions [28], it is equally applicable to wave functions with other forms, including explicitly-correlated wave functions.

In this manuscript, we thus employ VMC to optimize explicitly correlated wave functions containing 7 and 10 parameters to describe the lowest quartet state of the Li isoelectronic sequence. We show that VMC is able to rapidly find and converge parameters to a set that minimizes the energy. We find that the optimal parameters in general fit to Padé functions of the nuclear charge within the error bars. Our VMC-optimized wave functions yield energies which reproduce at least 99.9% of the most accurate Hylleraas results. Our work therefore demonstrates the potential that VMC methods have for optimizing explicitly-correlated wave functions of difficult to describe, higher angular momentum states.

2. Wave functions used to describe the Li isoelectronic series $1s2s2p$ quartet state

Members of the lithium isoelectronic sequence contain a total of four charged subatomic particles – three electrons and one nucleus – interacting via the Coulomb potential. Since the motion of the nucleus is much slower than that of the electrons, in the limit of infinite mass, it can be assumed to be a fixed, positively-charged center, effectively reducing the problem from twelve to nine degrees of freedom. We illustrate such a system, its parameters, and the notation we later employ for those parameters in Fig. 1.

Based on the conventional atomic shell model, the ground state with total spin $S = 1/2$ possesses two electrons that occupy the same orbital and a third that occupies a different, higher-energy orbital. However, for quartet states with total spin $S = 3/2$, all of the electrons lie in different orbitals. This state can be harder to describe because of its higher-spin and open shell character.

To design an explicitly-correlated wave function that can describe this state, we first consider the physics of these systems when the positive nuclear charge, Z, goes to infinity $Z \to \infty$. In this limit, nuclear–electron interactions dominate and the electron–electron interactions can be neglected, reducing the problem to that of three hydrogen electrons in three different orbitals. In this limit, there exists an exact solution to the Schrödinger equation in the form of an anti-symmetrized product of three Coulomb orbitals

$$\begin{aligned} 1s_1 &\sim e^{-\alpha_1 r_1} \\ 2s_2 &\sim (1 + a r_2) e^{-\alpha_2 r_2} \\ 2p_3 &\sim r_3 \cos\theta_3 e^{-\alpha_3 r_3} \\ \psi_0 &\sim 1s_1 2s_2 2p_3 \\ \psi_0 &\sim (1 + a r_2)(r_3 \cos\theta_3) \times \\ &\quad e^{-\alpha_1 r_1 - \alpha_2 r_2 - \alpha_3 r_3}, \end{aligned} \tag{1}$$

where $\alpha_1 = Z$, $a = -Z/2$ and $\alpha_2 = \alpha_3 = Z/2$ [29]. r_i and r_{ij} are the relative distances defined in Fig. 1.

Motivated by Eq. (1), we follow a recipe for designing compact wave functions described in our previous work [30–32]. The total wave function, Ψ, is the antisymmetrized product of the spatial wave function, ψ, and the spin function, χ, $\Psi = \mathcal{A}(\psi\chi)$. The antisymmetrization operator is defined as

$$\mathcal{A} = 1 - \hat{P}_{12} - \hat{P}_{13} - \hat{P}_{23} + \hat{P}_{231} + \hat{P}_{312},$$

where $\hat{P}_{ij}$ permutes the electrons $i \leftrightarrow j$ and $\hat{P}_{ijk}$ permutes the (ijk) indices. Since the spin function for the quartet state is totally symmetric,

[1] Note that these explicitly-correlated methods differ from the explicitly-correlated F12 and R12 methods of recent note in the literature [18].

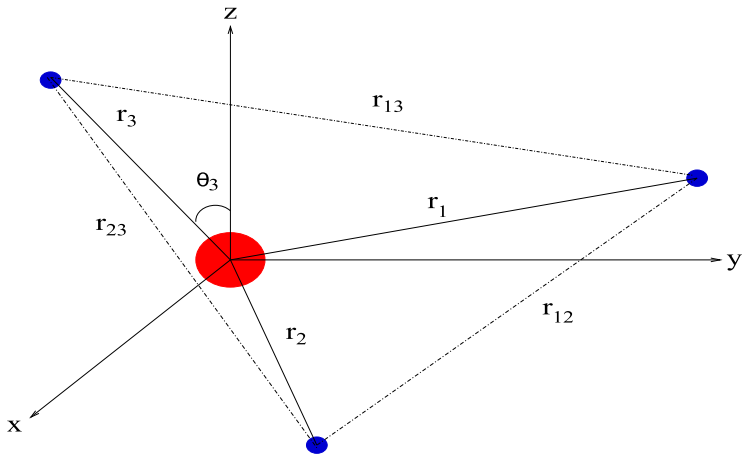

Fig. 1. Geometry of a representative member of the lithium isoelectronic sequence consisting of three electrons (blue) and a nucleus (red). Key distances and bond angles, some of which are used in our explicitly correlated wave functions, are denoted in black.

$\chi = \alpha\alpha\alpha$, where α denotes the spin-up function, the anti-symmetrization ends up being only performed on the spatial term ψ. The spatial wave function we propose has the following form

$$\psi = (1 + ar_2)\left(r_3 \cos\theta_3\right) \times e^{-\alpha_1 r_1 - \alpha_2 r_2 - \alpha_3 r_3 + \alpha_{12} r_{12} + \alpha_{13} r_{13} + \alpha_{23} r_{23}}, \tag{2}$$

where α_i with $i = 1,2,3$, α_{ij} with $j > i = 1,2,3$, and a are free variational parameters. The nonlinear variational parameters α_i and α_{ij} represent screening/antiscreening factors for the Coulomb charges in the nucleus–electron and electron–electron interactions, respectively. The factor depending on $\cos\theta_3$ leads to the required odd parity, while the total angular momentum $L = 1$ guarantees orthogonality with the $1s2s3s$ quartet state. We denote the wave function in Eq. (2), containing seven variational parameters, as Ansatz A.

As a generalization, we also consider inserting the following rational expressions into the exponents of the orbitals

$$\alpha_i r_i \to \alpha_i \hat{r}_i = \alpha_i r_i \frac{1 + c_i r_i}{1 + d_i r_i}. \tag{3}$$

These terms interpolate the effective Coulomb charges between their values at small and large distances. Calculations show that only some terms in the exponential lead to a significant difference, beyond statistical fluctuations, when replaced by Eq. (3). This leads to Ansatz B, given by

$$\psi = (1 + ar_2)\left(r_3 \cos\theta_3\right) \times e^{-\alpha_1 r_1 - \alpha_2 r_2 - \alpha_3 \hat{r}_3 + \alpha_{12} \hat{r}_{12} + \alpha_{13} r_{13} + \alpha_{23} r_{23}}, \tag{4}$$

which has 11 variational parameters. Our variational calculations show that α_3 can be fixed to $Z/2$, with no impact on the variational energy, effectively reducing the number of variational parameters to 10. This can be understood because, upon introducing the substitution $\alpha_3 r_3 \to \alpha_3 \hat{r}_3$, the screening charge of the nucleus as seen from the third electron at short distances is Z, leading $\alpha_3 \to Z/2$ according to Eq. (1).

Given these numbers of parameters, in the following, we optimize the parameters for the 7-parameter Ansatz A and the 10-parameter Ansatz B using Variational Monte Carlo.

3. Variational Monte Carlo

Variational Monte Carlo [26,27,33] is based upon the variational principle, which states that the variational energy of a system is given by

$$E_v = \frac{\langle\Psi|\hat{H}|\Psi\rangle}{\langle\Psi|\Psi\rangle} = \frac{\sum_\sigma \int d\mathbf{R} \Psi^\dagger(\mathbf{R},\sigma)\hat{H}\Psi(\mathbf{R},\sigma)}{\sum_\sigma \int d\mathbf{R} \Psi^\dagger(\mathbf{R},\sigma)\Psi(\mathbf{R},\sigma)} \geq E_0, \tag{5}$$

where $\mathbf{R} = \{\mathbf{r}_1, \mathbf{r}_2, \mathbf{r}_3\}$ and $\sigma = \sigma_1, \sigma_2, \sigma_3$ denote the positions and spins of the three particles (here, electrons), respectively, and E_0 is the exact ground state energy. The variational energy, E_v is estimated via the numerical evaluation of a nine-dimensional integral over the nine particle positions which can be performed via Monte Carlo methods.

To make Eq. (5) more directly amenable to Monte Carlo sampling, it can be rewritten as

$$E_v = \frac{\sum_\sigma \int d\mathbf{R} P(\mathbf{R},\sigma) \frac{\hat{H}\Psi(\mathbf{R},\sigma)}{\Psi(\mathbf{R},\sigma)}}{\sum_\sigma \int d\mathbf{R} P(\mathbf{R},\sigma)}, \tag{6}$$

where $P(\mathbf{R},\sigma)$ is a probability distribution of the form $P(\mathbf{R},\sigma) = \Psi^\dagger(\mathbf{R},\sigma)\Psi(\mathbf{R},\sigma)$. The quantity $\frac{\hat{H}\Psi(\mathbf{R},\sigma)}{\Psi(\mathbf{R},\sigma)}$ is known as the local energy, E_L. In the VMC method, P is sampled to generate a set of N configurations in $\{\mathbf{R},\sigma\}$ space that are used to estimate the integral above. A common way to sample such configurations is provided by the Metropolis algorithm. The spin variable, σ, can be integrated out analytically, both in the numerator and denominator of Eq. (6). This is because, for quartet states, there is only one spin function corresponding to the total spin $S = 3/2$ and projection S_z, on which the Hamiltonian does not act. The local energy is then evaluated based upon the configurations sampled and averaged to approximate the variational energy.

Other expectation values can also be calculated within the VMC framework by replacing the local energy in Eq. (6) by the quantity of interest. In particular, we are interested in computing the following ratio between expectation values

$$C_{Ne} = \frac{\langle \delta(\mathbf{r}_i) \frac{\partial}{\partial r_i} \rangle}{\langle \delta(\mathbf{r}_i) \rangle}, \tag{7}$$

in order to estimate the cusp condition $C_{Ne} \approx Z$, as a measure of the quality of the wave function in the vicinity of the Coulomb singularities.

The accuracy of the variational energy and other quantities so obtained depends upon the wave function parameterization, which can be optimized as described below. For a more detailed review of the VMC method, we refer the reader to Refs. [26,27,33–35].

4. Optimization of the wave function ansatz

In order to reach the lowest variational energy possible given the wave function ansatz, the wave function's parameters must be optimized. This can be achieved by performing gradient descent based upon the variational energies obtained using the VMC sampling described above. The derivative of the energy with respect to the variational parameters p is given by [27]

$$\frac{\partial\langle\hat{H}\rangle}{\partial p} = \frac{\langle\Psi|\Psi\rangle \frac{\partial}{\partial p}\langle\Psi|\hat{H}|\Psi\rangle - \langle\Psi|\hat{H}|\Psi\rangle \frac{\partial}{\partial p}\langle\Psi|\Psi\rangle}{\langle\Psi|\Psi\rangle^2}$$

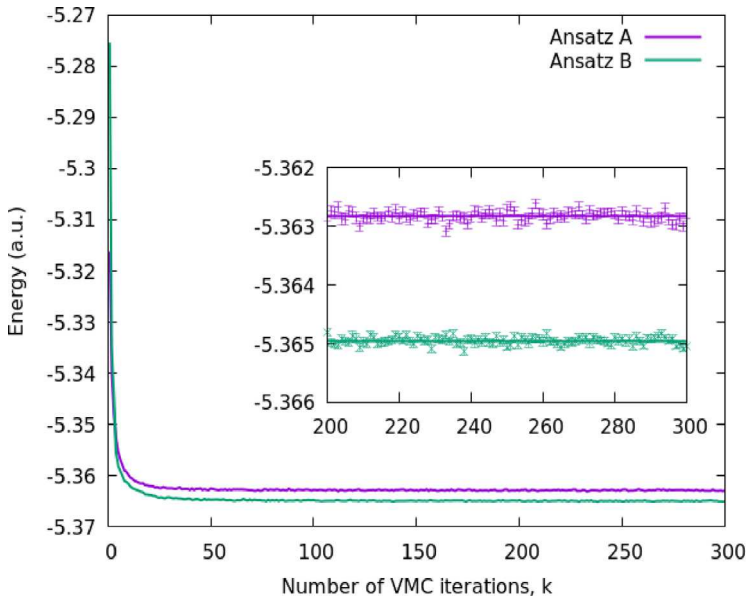

Fig. 2. Energy of neutral Lithium in the $1s2s2p$ state as a function of the number of VMC iterations. Ansatz A energies and error bars are given in purple, while Ansatz B energies and error bars are given in green.

$$= \frac{\langle \partial_p \Psi | \hat{H} | \Psi \rangle + h.c.}{\langle \Psi | \Psi \rangle} - \langle \hat{H} \rangle \frac{\langle \partial_p \Psi | \Psi \rangle + h.c.}{\langle \Psi | \Psi \rangle} \tag{8}$$

Within the framework of VMC, we can calculate the derivatives in Eq. (8) using the equations [36]

$$\langle \hat{H} \rangle = \int \Psi^* \Psi \frac{\hat{H}\Psi}{\Psi} d\mathbf{R} = \int P(\mathbf{R}) E_L d\mathbf{R} \tag{9}$$

$$\langle \Psi | \partial_p \Psi \rangle = \int \Psi^* \Psi \frac{\partial_p \Psi}{\Psi} d\mathbf{R} = \int P(\mathbf{R}) F_L^p d\mathbf{R} \tag{10}$$

$$\langle \Psi | \hat{H} | \partial_p \Psi \rangle = \int \Psi^* \Psi \frac{\hat{H}\partial_p \Psi}{\Psi} d\mathbf{R} = \int P(\mathbf{R}) G_L^p d\mathbf{R}, \tag{11}$$

and evaluate the related integrals in one single calculation based on the Metropolis algorithm. We update the variational parameters p_{k+1} corresponding to the next iteration $k+1$ according to

$$p_{k+1} = p_k + \lambda_p \left(\frac{\partial \langle \hat{H} \rangle}{\partial p} \right)_k \tag{12}$$

where λ_p is an update rate which can be tuned for each variational parameter p in order to accelerate convergence.

5. Numerical details

To perform these VMC calculations, we wrote a Fortran-based code which optimizes wave functions in the form of Ansatz A (Eq. (2)) and Ansatz B (Eq. (4)) for lithium in its $1s2s2p$ quartet state. The optimization is carried out using the gradient descent method during which VMC is used to determine energies and gradients and stochastic gradient is iteratively used to update the parameters based upon these gradients. One iteration typically consists of 10^7 Metropolis steps. We view the wave function as optimized when the variational energy converges, i.e., does not further decrease, within statistical error bars, after 50 consecutive iterations. It is worthwhile to mention that the optimization can be started from different starting configurations of parameters to reduce the risk of finding a local minimum. The number of iterations needed to obtain energy convergence, i.e., when all variational parameters reach equilibrium and oscillate around their optimal values, highly depends on the descent parameter λ. Practical calculations show that some parameters reach equilibrium faster than others. Thus, we used different descent parameters for the different wave function parameters: $\lambda_{\alpha_i} = 2$ for $i = 1, 2, 3$, $\lambda_{\alpha_{ij}} = 0.2$ for $i < j$, and $\lambda_a = 10$. With these descent parameters, we observe convergence after ~50 iterations (see Fig. 2, for instance) and compute expectation values after this convergence has been attained. We wrote a specialized code to estimate the cusp parameter Eq. (7) once parameters have been optimized and expectation values have been converged.

6. Results

6.1. Variationally optimized wave functions and energies

Using the VMC approach described above, we optimized the explicitly-correlated wave functions given by Ansatz A (Eq. (2)) and Ansatz B (Eq. (4)) for neutral lithium and its isoelectronic sequence with nuclear charges between $3 - 10$ in the $1s2s2p$ state. A good initial set of variational parameters is that given by the analytical solution for the infinite nuclear charge (Eq. (1)), i.e., $\alpha_1 = Z$, $a = -Z/2$, $\alpha_2 = \alpha_3 = Z/2$, and $\alpha_{ij} = 0$. For instance, we show in Fig. 2 the energy for the neutral Li as a function of the VMC iterations. One can see that the energy decreases monotonically following the gradient descent optimization and converges for both ansatz in less than 50 iterations. Once the energy has converged within statistical error bars, estimates of the variational energy and cusp parameters are made.

These results are presented in Table 1 alongside the most accurate published theoretical results produced by Hylleraas CI (HCI) for the electronic Schrödinger equation with fixed nuclei [13]. We also include the experimental energies for the ground states, which contain relativistic and QED contributions as well as non-BO effects, in Table 1. One can notice that the difference between the HCI and experimental results appears beyond the fourth significant digit. However, the energies free of corrections are correctly reproduced by both ansatz. Significant differences, beyond statistical errors, appear between the energies predicted by Ansatz A and B for small nuclear charges, but disappear for larger values. The percent energy differences between Ansatz A's predictions and the exact energies lie within roughly 0.01–0.1% for $Z = 3 - 10$, while those for Ansatz B lie within 0.01–0.05% over the same range of Z values. The percentage of correlation energy recovered by our Ansatz is also included in Table 1 since this can be a more sensitive measure of errors that also provides insight into how significant a role correlation plays in the electronic structure of the species studied. To obtain the Hartree Fock energies, we use the form of the wave function given by Ansatz A but set the two-body Jastrow terms to zero by setting $\alpha_{ij} = 0$ for $i, j = 1, 2, 3$. The energies obtained

Table 1
Variational energies, E_v, in Hartrees and cusp parameter, C_{Ne}, in atomic units for Li-like ions in the $1s2s2p$ quartet state in comparison with the most accurate previous results, E_{HCI} (Hylleraas CI) [13]. Experimental values, E_{exp} [37], that contain relativistic and QED contributions are also included for nuclear charges $Z = 3 - 5$. The last digit in parentheses indicates the statistical error. In the last column, the energies predicted using the Majorana formula, E_M, are noted.

	Ansatz A			Ansatz B					
Z	E_v	C_{Ne}	$E_{corr}(\%)$	E_v	C_{Ne}	$E_{corr}(\%)$	E_{HCI}	E_{exp}	E_M
3	−5.3629(1)	2.99199(3)	62	−5.3650(1)	2.99259(3)	77	−5.3680	−5.3660	−5.362
4	−10.0610(2)	3.97481(7)	63	−10.0631(2)	3.97700(2)	77	−10.0666	−10.0675	−10.064
5	−16.2617(4)	4.95491(9)	64	−16.2636(4)	4.95798(9)	76	−16.2676	−16.2714	−16.265
6	−23.9636(6)	5.9325(1)	64	−23.9653(6)	5.9375(1)	74	−23.9696		−23.967
7	−33.1659(8)	6.9103(2)	63	−33.1673(8)	6.9119(2)	71	−33.1720		−33.168
8	−43.868(1)	7.8865(3)	59	−43.870(1)	7.8912(3)	71	−43.8748		−43.870
9	−56.070(2)	8.8616(4)	58	−56.072(2)	8.8680(4)	69	−56.0777		−56.071
10	−69.773(5)	9.8358(5)	54	−69.773(5)	9.8417(5)	54	−69.7808		−69.773

using this form coincide with those reported in Ref. [10] to four digits for neutral lithium. From the Table, we observe that, for small nuclear charges, our Ansatz is capable of recovering 62 and 77 percent of the correlation energy, respectively. It is worthwhile to mention that this quartet state ($S = 3/2$) is more weakly correlated than the doublet states ($S = 1/2$) in which two electrons lie in the same orbital; that is, the Hartree–Fock energy of the quartet is closer to the exact energy than that of the doublet states. For large nuclear charge, the correlation energy vanishes because, for infinite nuclear charge, Eq. (1) is the exact solution.

6.2. Variationally-optimized cusp parameters

The cusp conditions (given by Kato's Theorem) establish that the exact wave function of a system composed of Coulombic charges should reproduce the condition given by Eq. (7) in order to remove divergences in the local energy at the electron–nucleus coalescence points [38]. Thus, beyond the energy, one observable of interest is the cusp parameter, C_{Ne}, which indicates how capable the electronic wave function is of removing the Coulomb singularity at the position of the nucleus. The accuracy with which the cusp parameter can be computed is also a good measure of the accuracy of the wave function given its sensitivity to the electronic structure around the nucleus. We find that 98%–99% of the cusp parameter is reproduced by both ansatz, indicating the high quality of the wave functions in the vicinity of the nucleus. Even though the difference between the Ansatz A and B energies is within statistical error bars for $Z = 10$, we find that the cusp condition is always better described by Ansatz B. Satisfying the cusp conditions is a relevant asset in quantum Monte Carlo calculations since it significantly reduces the variance of the local energy during random sampling [39]. It is also known that fulfilling cusp conditions is necessary to obtain an adequate description of the electron energy distributions in double photoionization [40].

6.3. The Majorana formula and parameter scaling

With optimized wave function parameters in hand, one may ask how these parameters scale with the nuclear charge. To more deeply appreciate how this scaling differs from previous analytical results, we first compare how our parameters vary with predictions from the Majorana Formula and perturbative treatments to it.

In his pioneering work that sought a simple, analytical expression for the wave function of helium in its ground state, E. Majorana noticed that the dominant contributions to the ground state energy of He-like atoms comes from a quadratic function of their nuclear charge. This led him to propose the Majorana Formula [41]

$$E_M = -\left(Z - \frac{5}{16}\right)^2 . \tag{13}$$

This formula can be derived analytically by taking the expectation value of the Hamiltonian with a wave function composed of the product of two 1s orbitals

$$\varphi = e^{-\alpha(r_1 + r_2)} \tag{14}$$

with a variational parameter α. After variational minimization, the optimal value of α as a function of the nuclear charge, Z, is given by

$$\alpha(Z) = Z - \frac{5}{16} . \tag{15}$$

Note that α varies linearly with the nuclear charge, as is also observed in our plots of our one-body variational parameters in Fig. 3. The Majorana Formula with its optimized α recovers roughly 98% of the exact energy of helium, an accuracy similar to that provided by Hartree–Fock theory.

Further corrections to the Majorana Formula can be obtained via the $1/Z$ expansion [41]. If the wavefunction in Eq. (14) is multiplied by an exponential factor $e^{\beta r_{12}}$, where r_{12} is the distance between the electrons and β another variational parameter, the error of the variational energy decreases to roughly 1%. Note that this exponential is similar in form to the electron–electron terms present in our Ansatz and these corrections can shed light on how we should expect our electron–electron parameters to scale. Although the integrals needed to estimate the expectation value of the Hamiltonian can be obtained analytically, the optimization of the variational parameters requires estimating the roots of a fifth-degree polynomial which can only be performed numerically [42]. However, one can observe that the following Padé approximant

$$\beta(Z) = \frac{a_0 + a_1 Z}{b_0 + b_1 Z} , \tag{16}$$

correctly describes the optimal values of β, found in Ref. [42], for nuclear charges between $Z = 2 - 20$. The fitting parameters are $a_0 = 1.16$, $a_1 = -3.11$, $b_0 = -2.11$, and $b_1 = 18.12$. Notice that linear functions are particular cases of Padé functions if $b_0 = 1$ and $b_1 = 0$.

In the last column of Table 1, we include the results provided by the Majorana Formula for the lithium 1s2s2p sequence to compare to our variational results. In Fig. 4, we plot (a) the Majorana Formula for the $1s2s2p$ state and (b-l) the optimized wavefunction parameters with error bars as a function of the nuclear charge alongside the fits (whose forms are specified in Table 2). It is evident from the plots that parameters α_1, α_2, and α_3 (plots c–e) scale roughly linearly with Z, which is in good agreement with Eq. (15). In these cases, the error bars are smaller than can readily be discerned (their exact values can be found in the Supplemental Materials). The other variational parameters are better approximated by Padé functions motivated by Eq. (16). The fits, including the evaluation of the Majorana Formula, are presented in Table 2.

Also, by analytic continuation of the Padé functions in Table 2, we were able to estimate the critical charge [32] $Z_c \sim 1.26 - 1.27$ (for which Ansatz A and B lose square normalizability), thus predicting the stability of the quartet state $1s2s2p$ for the anion He^- ($Z = 2$).

7. Conclusions

In summary, in this manuscript, we optimized ultra-compact, explicitly-correlated wave functions for neutral lithium and its iso-electronic sequence with nuclear charges $Z = 3$ to $Z = 10$ in the

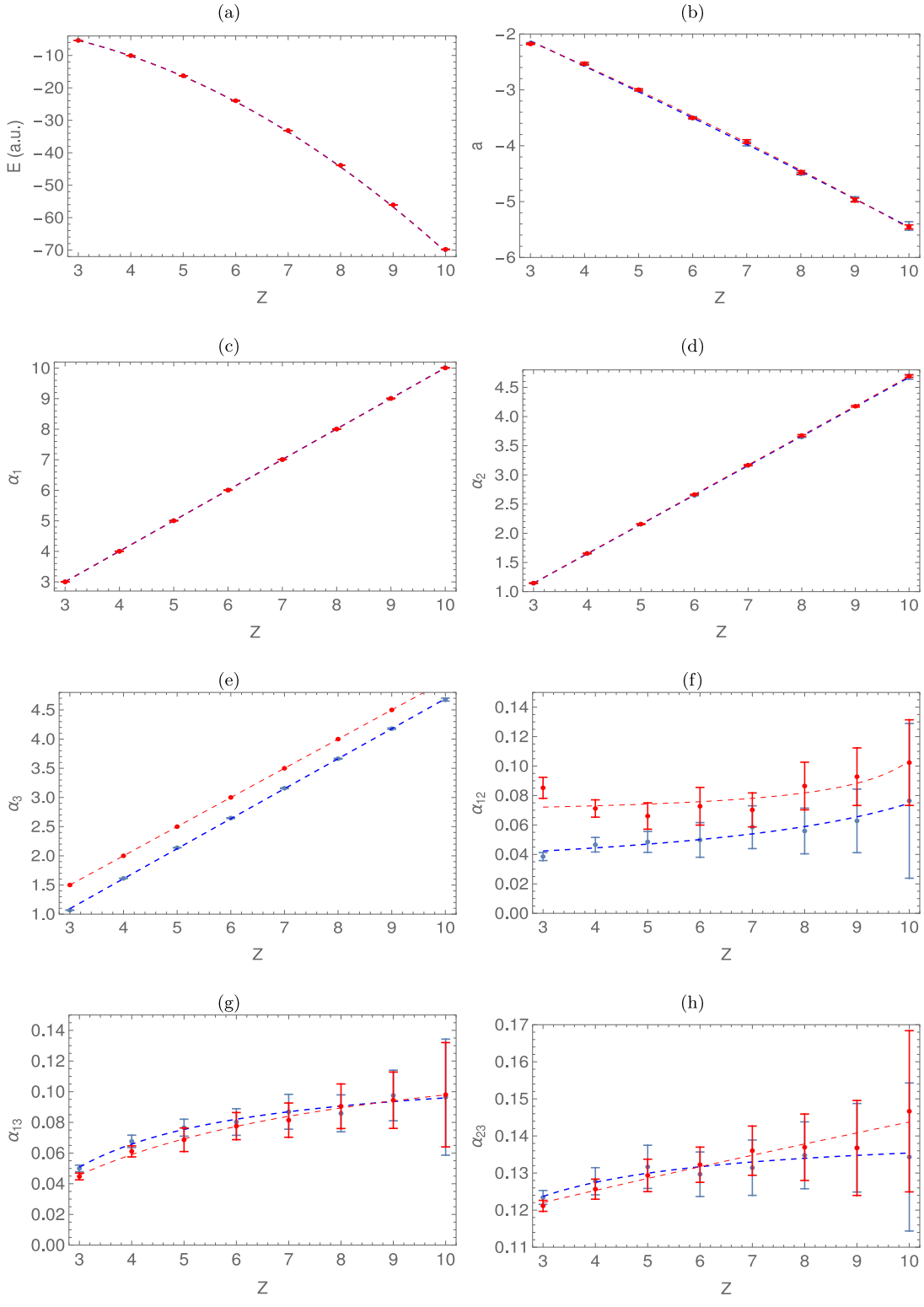

Fig. 3. Energy and variational parameters as a function of the nuclear charge Z. The dashed lines correspond to fits to Ansatz A in blue and Ansatz B in red. Error bars are sometimes smaller than the width of the symbol.

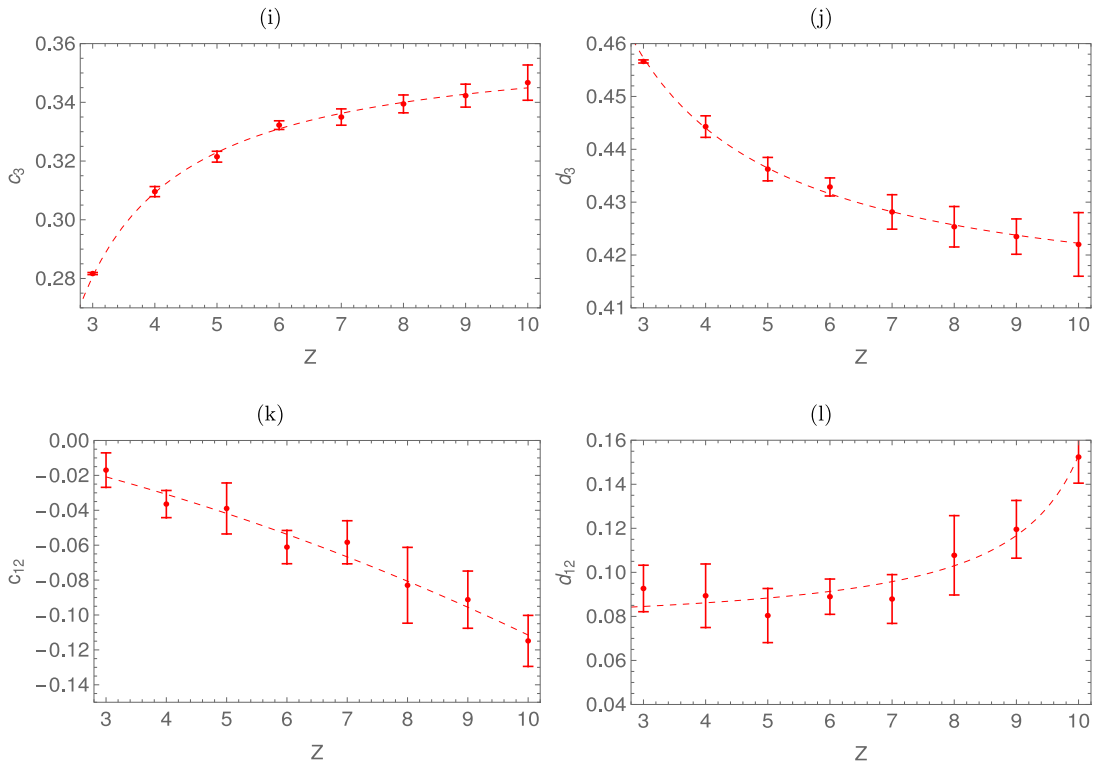

Fig. 4. Continuation of Fig. 3.

Table 2
Fits to the energy (Majorana formula energy given in first row) and to the optimal variational parameters as a function of the nuclear charge.

Ansatz A	Ansatz B
$E(Z) = -0.2549 + 0.5483Z - \frac{3}{4}Z^2$	$E(Z) = -0.2580 + 0.5486Z - \frac{3}{4}Z^2$
$a(Z) = \frac{-0.8257 - 0.4153Z}{1 - 0.0087Z}$	$a(Z) = \frac{-0.9244 - 0.3713Z}{1 - 0.0153Z}$
$\alpha_1(Z) = 0.0012 + 1.0011Z$	$\alpha_1(Z) = -0.0005 + 1.0008Z$
$\alpha_2(Z) = -0.3686 + 0.5040Z$	$\alpha_2(Z) = -0.3715 + 0.5059Z$
$\alpha_3(Z) = -0.5324 + 0.5250Z$	$\alpha_3(Z) = \frac{Z}{2}$
$\alpha_{12}(Z) = \frac{0.0376 - 0.0013Z}{1 - 0.0664Z}$	$\alpha_{12}(Z) = \frac{0.0703 - 0.0057Z}{1 - 0.0869Z}$
$\alpha_{13}(Z) = \frac{0.5278 - 0.2835Z}{1 - 2.5281Z}$	$\alpha_{13}(Z) = \frac{-0.0388 + 0.0408Z}{1 + 0.2769Z}$
$\alpha_{23}(Z) = \frac{0.1038 + 0.0477Z}{1 + 0.3278Z}$	$\alpha_{23}(Z) = \frac{0.1118 + 0.0046Z}{1 + 0.0099Z}$
	$c_3(Z) = \frac{0.4902 - 0.3114Z}{1 - 0.8607Z}$
	$d_3(Z) = \frac{0.0726 - 1.0879Z}{1 - 2.6594Z}$
	$c_{12}(Z) = \frac{0.0044 - 0.0078Z}{1 - 0.0344Z}$
	$d_{12}(Z) = \frac{0.0813 - 0.0065Z}{1 - 0.0892Z}$

lowest quartet state $1s2s2p$ using the variational Monte Carlo method. We found that VMC yielded accurate wave function parameters that resulted in energies competitive with the accuracy of energies produced by CI (~77% of the correlation energy for small nuclear charges). We also fit these parameters to linear and Padé functions of the nuclear charge, revealing how they change with charge. Uniquely, we have used our VMC approach to study the critical charges of this isoelectronic series, showing that VMC can reproduce 98% or more of the predicted critical charges. The estimate of critical charges in small atomic systems and their behavior close to the threshold is an active area of research [43–45]. Our results illustrate the power of VMC when it is used along with explicitly-correlated wave functions and indicate that VMC is able to reproduce 99.9% of the exact energy with only 10 nonlinear variational parameters for the problems studied here. This work moreover highlights the efficiency with which VMC can evaluate energies and other integrals needed to perform wave function optimization when the number of degrees of freedom is larger than 8, at which point MC integration becomes more efficient than other integration methods.

We can further improve the accuracy of our wave functions in two ways: by using (i) a linear superposition [17] of wave functions in the form of Ansatz A with different variational parameters,[2] or (ii) our optimized wave functions in tandem with other projector QMC methods (typically Diffusion Monte Carlo) that can further improve their structures and minimize their energies. VMC-optimized wave functions are often used as reliable trial wave functions that other, even higher accuracy QMC methods can then refine.

However, before adding more electrons to the atomic system, it is also worth examining explicitly-correlated wave functions for doublet excited states with total spin $S = 1/2$, where the symmetrization of the total wave function $\mathcal{A}(\phi\chi)$, including the Jastrow factor, is not trivial. Spin contamination will appear for any state if the wave function is not properly antisymmetrized [46].

Furthermore, explicitly-correlated wave functions are useful as starting points to explore the electronic structure of atoms embedded in media [47] or in magnetic fields. Even if the magnetic field is on the order typical of those observed in neutron stars, 10^{12}–10^{13} G, and magnetic white dwarfs, 10^{8}–10^{10} G, the wave function can be approximated by taking the product of the explicitly-correlated wave function in the zero field case and the Landau orbitals for each electron [48,49]. We look forward to the further development and application of these algorithms to tackle these exciting challenges.

[2] In Ref. [17], the authors found that the energy of the He ground state converges taking the sum of only four compact, explicitly-correlated wave functions.

CRediT authorship contribution statement

D.J. Nader: Conceptualization, Formal analysis, Investigation, Methodology, Software, Writing – original draft. **B.M. Rubenstein:** Funding acquisition, Investigation, Project administration, Resources, Supervision, Visualization, Writing – review & editing.

Declaration of competing interest

The authors declare that they have no known competing financial interests or personal relationships that could have appeared to influence the work reported in this paper.

Data availability

All codes, scripts, suplemental formulas and data needed to reproduce the results in this manuscript are available online https://github.com/djuliannader/VMCLitio.

Acknowledgments

D.J.N. thanks the kind hospitality of the Brown University Department of Chemistry and A.V. Turbiner and J.C. Lopez Vieyra for insightful discussions. D.J.N. was supported by Fulbright COMEXUS Project NO. P000003405, while B.R. acknowledges support from NSF CTMC CAREER Award 2046744. This research was conducted using computational resources and services at the Center for Computation and Visualization, Brown University.

Appendix A. Supplementary data

Supplementary material related to this article can be found online at https://doi.org/10.1016/j.cplett.2024.141091.

References

[1] A.J. Thakkar, T. Koga, T. Tanabe, H. Teruya, Compact Hylleraas-type wavefunctions for the lithium isoelectronic sequence, Chem. Phys. Lett. 366 (1) (2002) 95–99.
[2] M.B. Ruiz, J.T. Margraf, A.M. Frolov, Hylleraas-configuration-interaction analysis of the low-lying states in the three-electron Li atom and Be^+ ion, Phys. Rev. A 88 (2013) 012505.
[3] V.A. Yerokhin, V. Patkóš, K. Pachucki, Atomic structure calculations of helium with correlated exponential functions, Symmetry 13 (7) (2021) 1246, arXiv:2107.06134 [physics.atom-ph].
[4] S. Mannervik, H. Cederquist, The quartet system of Li I, Phys. Scr. 27 (3) (1983) 175.
[5] J.-J. Hsu, K.T. Chung, K.-N. Huang, Term values of 1s2s2p $^4P^\circ$ for lithiumlike ions, Phys. Rev. A 44 (1991) 5485–5491.
[6] S. Bubin, O.V. Prezhdo, Excited states of positronic lithium and beryllium, Phys. Rev. Lett. 111 (2013) 193401.
[7] T. Yamashita, Y. Kino, Calculation of resonance states of positronic lithium atom*, Eur. Phys. J. D 70 (9) (2016) 190.
[8] D. Bressanini, Positron binding to lithium excited states, Phys. Rev. Lett. 109 (2012) 223401.
[9] C.F. Bunge, A.V. Bunge, Configuration-interaction studies of transition energies and oscillator strengths for the lowest quartet states of neutral lithium, Phys. Rev. A 17 (1978) 822–828.
[10] S. Lunell, N.H.F. Beebe, Hartree-Fock and configuration interaction calculations of hyperfine constants in quartet states of three-electron atoms, Phys. Scr. 15 (4) (1977) 268.
[11] J.-J. Hsu, K.T. Chung, K.-N. Huang, $^4P^o$ Series of lithium, Phys. Rev. A 49 (1994) 4466–4472.
[12] S. Larsson, R. Crossley, Calculation of the 4s4p0 spectrum of lithiumlike ions by the Hylleraas method, Int. J. Quantum Chem. 22 (4) (1982) 837–849, URL https://onlinelibrary.wiley.com/doi/abs/10.1002/qua.560220413.
[13] R. Barrois, S. Bekavac, H. Kleindienst, Nonrelativistic energies for the lowest 4P° states of the Li isoelectronic series, Chem. Phys. Lett. 268 (5) (1997) 531–534.
[14] F.W. King, High-precision calculations for the ground and excited states of the lithium atom, in: B. Bederson, H. Walther (Eds.), in: Advances in Atomic, Molecular, and Optical Physics, vol. 40, Academic Press, 1999, pp. 57–112.
[15] D. Bressanini, G. Morosi, A compact boundary-condition- determined wavefunction for two-electron atomic systems, J. Phys. B: At. Mol. Opt. Phys. 41 (14) (2008) 145001.
[16] C.W. David, Compact $10.2em0ex^1S$ helium wave functions, Phys. Rev. A 74 (2006) 014501.
[17] F.E. Harris, V.H. Smith, Highly compact wave functions for He-like systems, J. Phys. Chem. A 109 (50) (2005) 11413–11416, PMID: 16354029.
[18] L. Kong, F.A. Bischoff, E.F. Valeev, Explicitly correlated R12/F12 methods for electronic structure, Chem. Rev. 112 (1) (2012) 75–107.
[19] S. Jones, D.H. Madison, Role of the ground state in electron-atom double ionization, Phys. Rev. Lett. 91 (2003) 073201.
[20] L.U. Ancarani, G. Gasaneo, A simple parameter-free wavefunction for the ground state of three-body systems, J. Phys. B: At. Mol. Opt. Phys. 41 (10) (2008) 105001.
[21] M.F. Ciappina, M. Schulz, T. Kirchner, Reaction dynamics in double ionization of helium by electron impact, Phys. Rev. A 82 (2010) 062701.
[22] M. Kircher, F. Trinter, S. Grundmann, G. Kastirke, M. Weller, I. Vela-Perez, A. Khan, C. Janke, M. Waitz, S. Zeller, T. Mletzko, D. Kirchner, V. Honkimäki, S. Houamer, O. Chuluunbaatar, Y.V. Popov, I.P. Volobuev, M.S. Schöffler, L.P.H. Schmidt, T. Jahnke, R. Dörner, Ion and electron momentum distributions from single and double ionization of helium induced by compton scattering, Phys. Rev. Lett. 128 (2022) 053001.
[23] D.H. Madison, D. Fischer, M. Foster, M. Schulz, R. Moshammer, S. Jones, J. Ullrich, Probing scattering wave functions close to the nucleus, Phys. Rev. Lett. 91 (2003) 253201.
[24] E. Bahati, H. Cherkani-Hassani, P. Defrance, J.J. Jureta, T. Kereselidze, Z. Machavariani, I. Noselidze, On the behaviour of the (e, 3e) total cross section for helium at high and intermediate energies, J. Phys. B: At. Mol. Opt. Phys. 38 (8) (2005) 1261.
[25] L. Kong, F.A. Bischoff, E.F. Valeev, Explicitly correlated R12/F12 methods for electronic structure, Chem. Rev. 112 (1) (2012) 75–107, PMID: 22176553.
[26] J. Toulouse, R. Assaraf, C.J. Umrigar, Chapter fifteen - introduction to the variational and diffusion Monte Carlo methods, in: P.E. Hoggan, T. Ozdogan (Eds.), Electron Correlation in Molecules – Ab Initio beyond Gaussian Quantum Chemistry, in: Advances in Quantum Chemistry, vol. 73, Academic Press, 2016, pp. 285–314.
[27] B. Rubenstein, Introduction to the variational Monte Carlo method in quantum chemistry and physics, in: J. Wu (Ed.), Variational Methods in Molecular Modeling, Springer Singapore, Singapore, 2017, pp. 285–313.
[28] R.J. Needs, M.D. Towler, N.D. Drummond, P.L. Ríos, Continuum variational and diffusion quantum Monte Carlo calculations, J. Phys.: Condens. Matter 22 (2) (2009) 023201.
[29] F.H. Stillinger, Ground-state energy of two-electron atoms, J. Chem. Phys. 45 (10) (1966) 3623–3631.
[30] A.V. Turbiner, J.C. Lopez Vieyra, J.C. del Valle, D.J. Nader, Ultra-compact accurate wave functions for He-like and Li-like iso-electronic sequences and variational calculus: I. Ground state, Int. J. Quantum Chem. 121 (8) (2021) e26586.
[31] A.V. Turbiner, J.C. Lopez Vieyra, J.C. del Valle, D. Julian Nader, Ultra-compact accurate wave functions for He-like and Li-like iso-electronic sequences and variational calculus: II. Spin-singlet (excited) and spin-triplet (lowest) states of helium sequence, Int. J. Quantum Chem. 122 (9) (2022) e26879.
[32] D. Julian Nader, J.C. del Valle, J.C. Lopez Vieyra, A.V. Turbiner, Ultra-compact accurate wave functions for He-like and Li-like iso-electronic sequences and variational calculus: III. Spin-quartet state (1s2s3s) of the lithium sequence, Int. J. Quantum Chem. 122 (17) (2022) e26952.
[33] W.M.C. Foulkes, L. Mitas, R.J. Needs, G. Rajagopal, Quantum Monte Carlo simulations of solids, Rev. Modern Phys. 73 (2001) 33–83.
[34] T. Pang, An Introduction to Quantum Monte Carlo Methods, 2016.
[35] B.L. Hammond, W.A. Lester, P.J. Reynolds, Monte Carlo Methods in Ab Initio Quantum Chemistry, World Scientific, 1994.
[36] J. Toulouse, C.J. Umrigar, Optimization of quantum Monte Carlo wave functions by energy minimization, J. Chem. Phys. 126 (8) (2007) 084102.
[37] A. Kramida, Yu. Ralchenko, J. Reader, NIST ASD Team, 2022, NIST Atomic Spectra Database (ver. 5.10), [Online]. Available: https://physics.nist.gov/asd [2022, March 24]. National Institute of Standards and Technology, Gaithersburg, MD..
[38] T. Kato, Fundamental properties of Hamiltonian operators of Schrödinger type, Trans. Amer. Math. Soc. 70 (1951) 195–211.
[39] P.-F. Loos, A. Scemama, M. Caffarel, Chapter five - Self-consistent electron–nucleus cusp correction for molecular orbitals, in: L.U. Ancarani, P.E. Hoggan (Eds.), State of the Art of Molecular Electronic Structure Computations: Correlation Methods, Basis Sets and more, in: Advances in Quantum Chemistry, vol. 79, Academic Press, 2019, pp. 113–132.
[40] E.G. Drukarev, Atomic physics: Computer calculations and theoretical analysis, Phys.-Usp. 50 (8) (2007) 835.
[41] S. Esposito, A. Naddeo, Majorana solutions to the two-electron problem, Found. Phys. 42 (12) (2012) 1586–1608, arXiv:1207.1666 [physics.hist-ph].
[42] P.C. Abbott, E.N. Maslen, A model wavefunction including electron correlation for the ground state of the helium isoelectronic sequence, J. Phys. B: Atomic Mol. Phys. 19 (11) (1986) 1595.
[43] H.G.A. Burton, Hartree–Fock critical nuclear charge in two-electron atoms, J. Chem. Phys. 154 (11) (2021) 111103.
[44] A.W. King, L.C. Rhodes, C.A. Readman, H. Cox, Effect of nuclear motion on the critical nuclear charge for two-electron atoms, Phys. Rev. A 91 (2015) 042512.

[45] H. Montgomery Jr., K. Sen, J. Katriel, Correlation effects close to the ground state critical charge of the two-electron atom, Chem. Phys. Lett. 782 (2021) 139030.
[46] C.-J. Huang, C. Filippi, C.J. Umrigar, Spin contamination in quantum Monte Carlo wave functions, J. Chem. Phys. 108 (21) (1998) 8838–8847, arXiv:https://pubs.aip.org/aip/jcp/article-pdf/108/21/8838/10790526/8838_1_online.pdf.
[47] S.B. Doma, M.A. Salem, K.D. Sen, Plasma confined ground and excited state helium atom: A comparison theorem study using variational Monte Carlo and Lagrange mesh method, Computation 9 (12) (2021).
[48] A.V. Turbiner, J.C.L. Vieyra, One-electron molecular systems in a strong magnetic field, Phys. Rep. 424 (6) (2006) 309–396.
[49] A.V. Turbiner, J.C. Lopez Vieyra, Stable He^- can exist in a strong magnetic field, Phys. Rev. Lett. 111 (2013) 163003.